REFERENCES

1. Senturia YD. The epidemiology of testicular cancer. *Br J Urol* 1987;60:285–291.
2. Mostofi FK, Sobin LH. International histological classification of tumours of the testis (no. 16). Geneva: WHO; 1977.
3. Garnick MB. Testicular cancer and other trophoblastic diseases. In: Isselbacher KJ, Braunwald E, Wilson JD, et al., eds. *Harrison's principles of internal medicine*, 13th ed. New York: McGraw-Hill; 1994:1858–1862.
4. Fernandez EB, Moul JW, Foley JP, Colon E, McLeod DG. Retroperitoneal imaging with third and fourth generation computed axial tomography in clinical stage I nonseminomatous germ cell tumors. *Urology* 1994;44:548–552.
5. Carlsson-Farrelly E, Boquist L, Ljungberg B. Accuracy of clinical staging in non-seminomatous testicular cancer—a single center experience of retoperitoneal lymph node dissection. *Scand J Urol Nephrol* 1995;29:501–506.
6. Otto T, Goepel M, Seeber S, Rübben H. Delayed retroperitoneal lymph node excision in treatment of advanced nonseminomatous germinal cell tumors. I. Intraoperative findings in marker converted tumor. *Urologe A* 1993;32:189–193.
7. Borchers H, Sohn M, Müller-Leisse C, Fischer N, Jakse G. Growing teratoma syndrome [Abstract]. *Onkologie* 1991;14(suppl 4):13.
8. Rigo P, Paulus P, Kaschten BJ, et al. Oncological applications of positron emission tomography with fluorine-18 fluorodeoxyglucose. *Eur J Nucl Med* 1996;23:1641–1674.
9. Wilson CB, Young HE, Ott RJ, et al. Imaging metastatic germ cell tumours with ^{18}FDG positron emission tomography: prospects for detection and management. *Eur J Nucl Med* 1995;22:508–513.
10. Stephens AW, Gonin R, Hutchins GD, Einhorn LH. Positron emission tomography evaluation of residual radiographic abnormalities in postchemotherapy germ cell tumor patients. *J Clin Oncol* 1996;14:1637–1641.
11. Wahl RL, Greenough R, Clark MF, Grossman HB. Initial evaluation of FDG/PET imaging of metastatic testicular neoplasms. *J Nucl Med* 1993;34:6P.
12. Harms W, Bares R, Kamps H, et al. Therapy control of metastatic testicular carcinoma with ^{18}FDG PET. *J Nucl Med* 1995;36:198P.
13. Reinhardt MJ, Müller-Mattheis V, Gerharz CD, Vosberg H, Ackermann R, Müller-Gärtner HW. FDG PET evaluation of retroperitoneal metastases of testicular cancer before and after chemotherapy. *J Nucl Med* 1997;38:99–101.
14. Cavalli F, Monfardini S, Pizzocaro G. Report on the international workshop on staging and treatment of testicular cancer. *Eur J Cancer* 1980;16:1367–1372.
15. Shepp LA, Vardi Y. Maximum likelihood reconstruction for positron emission tomography. *IEEE Trans Med Imaging* 1982;2:113–122.
16. Bares R, Klever P, Hauptmann S, et al. Fluorine-18 fluorodeoxyglucose PET in vivo evaluation of pancreatic glucose metabolism for detection of pancreatic cancer. *Radiology* 1994;192:79–86.
17. Thill R, Cremerius U, Sabri O, et al. Quantitative criteria in ^{18}F-FDG PET for malignant lymphoma to evaluate cytostatic therapy. A follow-up study. In: *Proceedings of the European Conference on Research and Application of Positron Emission Tomography in Oncology*. Groningen; 1996:12–14.
18. Warren GP, Einhorn LH. Gallium scans in the evaluation of residual masses after chemotherapy for seminoma. *J Clin Oncol* 1995;13:2784–2788.
19. Janus T, Kim E, Tilbury R, Bruner J, Yung W. Use of ^{18}F-fluorodeoxyglucose positron emission tomography in patients with primary malignant brain tumors. *Ann Neurol* 1993;33:540–548.
20. Minn H, Paul R, Ahonen A. Evaluation of treatment response to radiation therapy in head and neck cancer with fluorine-18 fluorodeoxyglucose. *J Nucl Med* 1988;29:1521–1525.
21. Price P, Jones T. Can PET be used to detect subclinical response to cancer therapy? *Eur J Cancer* 1995;31A:1924–1927.
22. Strauss LG. Fluorine-18 deoxyglucose and false-positive results: a major problem in the diagnosis of oncological patients. *Eur J Nucl Med* 1996;23:1409–1415.
23. Kubota R, Yamada S, Kubota K, Ishiwata K, Tamahashi N, Ido T. Intratumoral distribution of fluorine-18-fluorodeoxyglucose in vivo: high accumulation in macrophages and granulation tissues studied by microautoradiography. *J Nucl Med* 1992; 33:1972–1980.

Hürthle Cell Tumor Dwelling in Hot Thyroid Nodules: Preoperative Detection with Technetium-99m-MIBI Dual-Phase Scintigraphy

Angelo Vattimo, Paolo Bertelli, Marcella Cintorino, Luca Burroni, Duccio Volterrani, Alessandra Vella and Stefano Lazzi

Nuclear Medicine Unit, Institute of Pathology, University of Siena, Siena, Italy

Single injection dual-phase scintigraphy (early and late acquisitions) with ^{99m}Tc-MIBI was used to differentiate benign and malignant hot thyroid nodules. **Methods:** Thirteen euthyroid and two hyperthyroid patients displaying a hot thyroid nodule on the ^{99m}Tc scan due to an autonomously functioning thyroid nodule (AFTN) underwent early (15–30 min) and late (3–4 hr) thyroid scintigraphy after the administration of 740–1000 MBq ^{99m}Tc-MIBI. Visual scoring was done to assess nodular tracer uptake and retention. In addition, the nodular-to-thyroid (N/T) uptake ratio in the early and late image and the washout rates (WO) from the nodule and thyroidal tissue were measured. All patients underwent thyroid surgery. **Results:** Histopathology revealed a Hürthle cell tumor in three nodules, a benign adenoma with oxyphilic metaplasia in two nodules and a benign adenoma without oxyphilic cells in the remaining 10 nodules. The Hürthle cell tumor nodules displayed intense and persistent uptake of ^{99m}Tc-MIBI (N/T was 2.81 ± 0.52 and 5.53 ± 1.06 in early and late images, respectively; WO from the nodule was 12.33 ± 0.47, WO from the thyroidal tissue was 22.00 ± 3.56). The benign nodules showed intense uptake in the early image and intense uptake to absent retention in the late image (N/T was 2.94 ± 1.31 and 1.62 ± 0.50 in the early and late images, respectively; WO from the nodule was 20.25 ± 2.92, WO from the thyroidal tissue was 20.33 ± 2.92). **Conclusion:** Single injection dual-phase ^{99m}Tc-MIBI scintigraphy of the thyroid with AFTN can identify nodules as a result of the activity of a Hürthle cell tumor, since these tumors cause intense and persistent tracer uptake in contrast with a benign AFTN.

Key Words: thyroid scintigraphy; technetium-99m-sestamibi; hot nodules; Hürthle cells tumor

J Nucl Med 1998; 39:822–825

The rate of malignancy in thyroid nodules is fortunately very low, representing about 6% of all nodules (*1,2*); however, the rate of malignancy is higher in those nodules where ^{99m}Tc or radioiodine demonstrate to be scintigrafically cold than in those that are found to be hot (*3–6*). These latter sometimes appear hot with ^{99m}Tc and cold with radioiodine, since this tracer is rapidly removed from such nodules because they either have lost their ability to organify the iodine (*7*) or may be autonomous and enact a rapid turnover of iodine (*8*). In such cases, some authors have suggested reimaging with radioiodine those nodules that appear hot with ^{99m}Tc (*3–6,9–12*). Others (*13*) claim that this procedure is not necessary since the risk of cancer in such nodules is very low, accounting for 4%–11% of all hot nodules (*14*). Papillary or follicular cancer have been found to coincide and be associated with hot nodules, rather than cause the hot nodule (*14*). When present, a Hürthle cell tumor was found in the histology of these surgical specimens (*14–16*). Since in such cases total thyroidectomy is mandatory, its preoperative detection is of paramount importance.

Received May 23, 1997; accepted Aug. 4, 1997.

For correspondence or reprints contact: Angelo Vattimo, MD, Nuclear Medicine Unit of the University of Siena, Le Scotte Hospital, Viale Bracci, 53100 Siena, Italy.

MATERIALS AND METHODS

Patients

The study was performed on 15 patients (6 women, aged 48–68 yr; 9 men aged 34–62 yr) who had displayed a hot thyroid nodule with suppressed extranodular tissue on ^{99m}Tc scintigraphy due to an autonomously functioning thyroid nodule (AFTN). These patients were scheduled for thyroid surgery. The hormonal thyroid status was assessed using commercially available kits. Informed patient consent, as part of the protocol approved by the ethical committee of our institution, was obtained from all patients.

Technetium-99m-MIBI Scintigraphy

Within a week of thyroid scintigraphy with ^{99m}Tc (185 MBq), all patients were imaged 15–30 min (early image) and 3–4 hr (late image) after the administration of 740–1000 MBq ^{99m}Tc-MIBI (Cardiolite, DuPont Pharma, North Billerica, MA; labeling efficiency >95%) without any specific preparation. Particular care was used in patient repositioning and to guarantee maximum comfort since the acquisition of each image required 10–20 min for a preset count of 50K. The images were acquired using a small field of view gamma camera fitted with a 2-mm pinhole collimator encompassing an area of 10 × 10 cm in 64 × 64 matrices; the images were stored on a hard disk for further processing.

Scintigraphic Data Processing

Both images were displayed together and manual regions of interest (ROIs) were drawn on the nodule, the contralateral thyroid tissue and the surrounding extrathyroidal tissue. After background subtraction, the counts in each ROI were corrected for the area of the ROI, acquisition time and ^{99m}Tc decay. In addition, the following indices were calculated: the nodular-to-normal thyroidal tissue ratio (N/T) for the early and late images and the washout rate (WO) (fraction of the tracer removed) from the nodule and WO from the normal thyroid tissue expressed as hr-1. Mann-Whitney (between groups) and Wilcoxon signed-rank (within groups) tests were used for statistical analysis.

Visual Interpretation

Two sets of images were arranged for visual interpretation: In the first set, the ^{99m}Tc and ^{99m}Tc-MIBI images were displayed at maximum expansion of the color scale for each image. In the second set, the late image with ^{99m}Tc-MIBI was presented after correction for time acquisition and ^{99m}Tc decay. The two sets of images were given separately, 2 wk apart, to two observers who were asked to score the extranodular uptake of ^{99m}Tc-MIBI and tracer uptake in the nodule in the early image and the retention in the late one as follows: 0 = no uptake or retention; 1 = faint uptake or retention; 2 = moderate uptake or retention; 3 = intense uptake or retention.

Histopathologic Data Analysis

Surgical specimens were analyzed using conventional histopathological methods. The nodules were diagnosed by the same pathologist who was also asked to score the oxyphilic cells as a percent of whole cellularity.

RESULTS

Histopathologic Data

In three patients, the entire nodule was found to be a Hürthle cell tumor (adenoma). In two patients, the nodules were diagnosed as benign adenoma with oxyphilic metaplasia, and the oxyphilic cellularity was scored as 10% and 20%. In the remaining 10 patients, the nodule was diagnosed as a benign adenoma without oxyphilic cells.

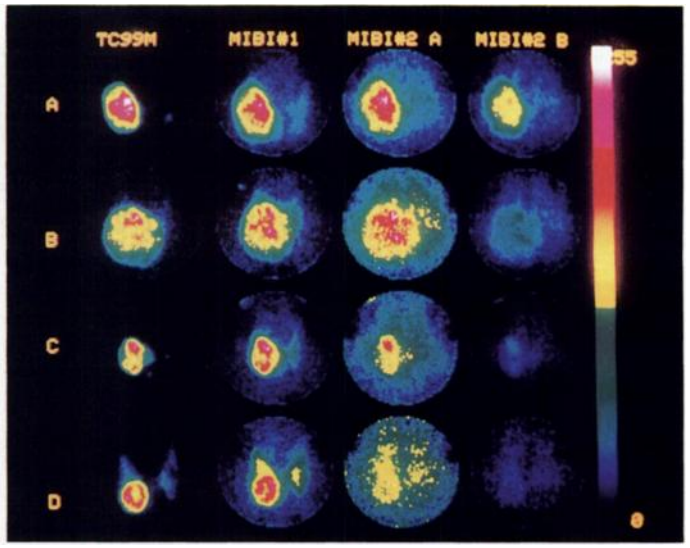

FIGURE 1. All nodules appearing hot on ^{99m}Tc scans (Patients 1, 3, 4 and 15) show intense uptake of ^{99m}Tc-MIBI with good visualization of extranodular tissue in early image (MIBI#1). In the late image, the retention was scored as intense (true retention) both in raw (MIBI#2 A) and in normalized images (MIBI#2 B) for Patient A; intense and moderate (true retention) for Patient B; intense and moderate (apparent retention) for Patient C and absence of retention for Patient D. Histology revealed a Hürthle cell tumor in Patients A and B; oxyphilic metaplasia in Patient C and the absence of oxyphilic cells in Patient D.

Visual Interpretation

The extranodular tissue was clearly delineated in all patients (Score 2–3) in the early image and disappeared completely in the late one (Score 0). The nodular tissue showed intense uptake in the early image in all patients; in the late image the retention was scored as intense in the 3 patients with a Hürthle cell tumor nodule, faint in 6, moderate in 3 and intense in 3 patients with a benign nodule in a full-color scale set. When corrected images were interpreted, the retention of Hürthle cell tumor nodules was scored as intense in 2 and moderate in 1. The retention of benign nodules was scored as intense in 2, moderate in 2, faint in 5 and absent in 3. The average scores were 3.00 ± 0.00 in the early image and 3.00 ± 0.00 and 2.67 ± 0.47 in the late images for Hürthle cell tumor nodules; 3.00 ± 0.00 in the early image and 1.75 ± 0.83 and 1.25 ± 1.01 in the late images for benign nodules. The differences proved to be statistically insignificant in Hürthle cell tumor nodules and statistically significant in benign nodules ($p < 0.01$). The differences between groups were found to be statistically insignificant for the early images and statistically significant for the late images.

Scintigraphic Data

Uptake Ratio. The early N/T ratios were 2.81 ± 0.52 and 2.94 ± 1.31 (p = ns); the late ones were 5.53 ± 1.06 and 1.62 ± 0.50 ($p < 0.01$) for Hürthle cell tumor and benign nodules, respectively. No statistically significant difference was found in Hürthle cell tumor nodules due to the small number of patients in the group, although the ratio increases. In contrast, the ratio statistically decreases ($p < 0.01$) the benign nodules.

Washout Rate. WO from the nodule was 12.33 ± 0.47 and 20.25 ± 2.92 ($p < 0.01$); WO from the thyroid tissue was 22.00 ± 3.56 and 20.33 ± 2.92 (p = ns) for Hürthle cell tumor and benign nodules, respectively. Although the WO from the nodule was lower than WO from the thyroid tissue in Hürthle cell tumor nodules, the difference was not statistically significant. In contrast, benign nodules had the same value (p = ns).

Figure 1 shows scintigraphic patterns in four representative patients. Table 1 shows the individual data of each patient.

DISCUSSION

It is generally accepted that thyroid nodules found to be hot on ^{99m}Tc scan, and especially those of the autonomous variety, are almost never malignant. In case of malignancy, such nodules appear cold on a radioiodine scan, so that some authors (*3–6*) suggest routine reimaging as an appropriate diagnostic approach. However, others believe that reimaging is not necessary since the risk of cancer is negligible and a discrepancy between ^{99m}Tc/radioiodine uptakes is far more likely to be caused by benign lesions than by malignancy (*13*). However, the risk of cancer still remains. In a series of 31 surgical patients with AFTN, David et al. (*14*) found hyperplasia in 19 nodules, associated carcinoma in 5 (4 papillary and 1 follicular), 1 Hürthle cell tumor and 1 case of thyroiditis. The follicular cancer was minimally invasive, while the cases of papillary cancer were small and occult. They arose in cold areas in proximity with the major hot nodule and were viewed as coincidental and associated with the nodule, rather than as arising or causing the hot nodule. Siddiqui et al. (*15*) reported on a Hürthle cell tumor in a euthyroid adolescent with AFTN. Moreover, Caplan et al. (*16*), from their observations and from a literature survey dating from 1950 through 1993 (*17–23*), identified 631 patients with Hürthle cell tumor: there were 561 adenomas and 70 carcinomas; thyroid scintigraphy with ^{99m}Tc or radioiodine performed on 317 patients revealed 267 cold nodules, 28 warm nodules, 14 hot nodules and 8 nodules with other scintigraphic aspects. These data demonstrate that Hürthle cell tumor may originate from thyroid nodules with variable capacity to concentrate ^{99m}Tc or radioiodine. Although the rate of Hürthle cell tumor was found to be high in cold nodules, a small percentage (13% about) was found in functioning nodules. The Hürthle cell tumor is a neoplasm composed predominantly or exclusively of follicular cells exhibiting oxyphilic features due to presence of abundant granular acidophilic cytoplasm, which is represented by crowded mitochondria and is responsible for ^{99m}Tc-MIBI uptake and retention (*24–26*). Since these cells have variable metabolic activity (*27–31*), the scintigraphic appearance displayed by ^{99m}Tc can vary, revealing cold, warm and hot nodules. However, the scintigraphic appearance with ^{99m}Tc-MIBI typically shows intense and persistent tracer uptake in contrast to other thyroid tumors (*32,33*). Technetium-99m-MIBI uptake by thyroid nodules is related to vascularity and cellularity (*34*), but its retention is mainly related to mithocondrial concentration (*24*) and secondarily to initial uptake. Since reactive oxyphilic cells are present in benign goiters and in chronic thyroiditis (*35–37*), their presence is unable to cause significant ^{99m}Tc-MIBI retention, as we found in two patients. In these patients, the retention of ^{99m}Tc-MIBI was found to be faint or moderate, the N/T ratio decreased and the WO from the nodule and thyroid tissue were of similar value (apparent retention), in contrast with Hürthle cell tumors, which exhibited an increase of N/T ratio and WO from the nodule lower than WO from the thyroid tissue (true retention). In these patients, histology revealed that oxyphilic cells were arranged in papillary or follicular patterns. Controversy arises from the view that all Hürthle cell tumors are malignant (carcinoma) or potentially malignant (adenoma) (*35,36*) and that the adenoma undergoes malignant transformation (*38*); thus, total thyroidectomy is suggested as the treatment of choice. Moreover, the carcinoma form has a high morbidity and mortality and, usually, does not concentrate radioiodine (*35,39–45*), except in a minority of local recurrences or metastases (*46–48*), which, in our opinion, could arise from hot nodules due to oxyphilic cells and benefit from radioiodine therapy. As such, a correct diagnosis of such tumors is of paramount importance and our data are promising in this regard.

CONCLUSION

Since ^{99m}Tc-MIBI was introduced to visualize extranodular inhibited thyroid tissue due to AFTN as an alternative to exogenous TSH stimulation (*34,49*), it has become possible reimage the thyroid 3–4 hr postinjection to assess the uptake and retention of ^{99m}Tc-MIBI in nodular tissue. Particular care must be taken in the visual evaluation of retention since apparent retention could be falsely interpreted, the increase in N/T ratio and WO from the nodule lower than WO from the thyroid tissue represent the indices of true retention. This approach allows nuclear medicine physicians to identify nodules caused by Hürthle cell tumors and enables surgeons to schedule total thyroidectomy. Finally, since this tumor maintains the ability to concentrate radioiodine, radiometabolic therapy could be considered after surgery and, especially, in recurrences.

ACKNOWLEDGMENTS

Financial support for this study was provided by grant Quota 60%, University of Siena, Siena, Italy.

REFERENCES

1. Werk EE, Vernon BM, Gonzalez et al. Cancer in thyroid nodules. A community hospital survey. *Arch Intern Med* 1984;144:474–476.
2. Belfiore A, Giuffrida D, La Rosa GL, et al. High frequency of cancer in cold thyroid nodules occurring at young age. *Acta Endocrinol* 1989;121:197–202.
3. Steinberg M, Cavalieri RR, Choy SH. Uptake of technetium-99m-pertechnetate in a primary thyroid carcinoma: need for caution in evaluating nodules. *J Clin Endocrinol* 1970;31:81–84.
4. Turner JW, Spencer RP. Thyroid carcinoma presenting as a pertechnetate "hot" nodule, but without ^{131}I uptake: case report. *J Nucl Med* 1976;17:22–23.
5. Quinn JL, Henkin RE. Scanning techniques to assess thyroid nodules. *Ann Rev Med* 1975;26:193–201.
6. O'Connor MK, Cullen MJ, Malone JF. A kinetic study of (^{131}I) iodine and ^{99m}Tc-pertechnetate in thyroid carcinomas to explain a scan discrepancy: case report. *J Nucl Med* 1977;18:796–798.
7. Demeester-Mirkine N, Van Sande J, Corvilain J, Dumont JE. Benign thyroid nodule with normal iodide trap and defective organification. *J Clin Endocrinol Metab* 1975;41:1169–1171.
8. Miller JM, Kasenter AG, Marks DS. Disparate imaging of the autonomous functioning thyroid nodule with ^{99m}Tc-pertechnetate and radioiodine. *Radiology* 1976;119:737–739.
9. Shambaugh GE, Quinn JL, Oyasu R, Freinkel N. Disparate thyroid imaging. Combined studies with sodium pertechnetate ^{99m}Tc and radioactive iodine. *JAMA* 1974;228:866–869.
10. Erjavec M, Movrin T, Auersperg M, Golouh R. Comparative accumunation of ^{99m}Tc and ^{131}I in thyroid nodules: case report. *J Nucl Med* 1977;18:346–347.
11. Massin JP, Planchon C, Accard JL, Perez R. Discordances scintigraphiques entrele technetium 99m et l'iode 131 dans l'etude des nodules thyroidiens. *Nouvelle Presse Med* 1977;6:97–100.
12. Szonyi G, Bowers P, Allwright S, et al. Comparative study of ^{99m}Tc and ^{131}I in thyroid scanning. *Eur J Nucl Med* 1982;7:444–446.
13. Kusic Z, Becker DV, Saenger EL, et al. Comparison of technetium-99m and iodine-123 imaging of thyroid nodules: correlation with pathological findings. *J Nucl Med* 1990;31:393–399.
14. David E, Rosen IB, Bain J, James J. Management of the hot thyroid nodule. *Am J Surg* 1995;170:481–483.
15. Siddiqui AR, Karanauskas S. Hürthle cell carcinoma in an autonomous thyroid nodule in an adolescent. *Pediatr Radiol* 1995;25:568–569.
16. Caplan RH, Abellera RM, Kisken WA. Hürthle cell neoplasms of the thyroid gland: reassessment of functional capacity. *Thyroid* 1994;4:243–248.
17. Rosen IB, Luk S, Katz I. Hürthle cell tumor behavior: dilemma and resolution. *Surgery* 1985;98:777–783.
18. Gosain AK, Clark OH. Hürthle cell neoplasm: malignant potential. *Arch Surg* 1984;119:515–519.
19. Saull SC, Kimmelman CP. Hürthle cell tumor of the thyroid gland. *Otolaryngol Head Neck Surg* 1985;93:58–62.
20. Gonzalez-Campora R, Herrero-Zapatero A, Lerma E, et al. Hürthle cell and mitochondria-rich cell tumors: a clinicopathological study. *Cancer* 1986;57:1154–1163.
21. Arganini M, Behar R, Wu TC, Straus F, et al. Hürthle cell tumors: a 25-year experience. *Surgery* 1986;100:1108–1114.
22. Bronner MP, LiVolsi VA. Oxyphilic (Askanazy/Hürthle cell) tumours of the thyroid: microscopic features predict biologic behavior. *Surg Pathol* 1988;1:137–150.
23. Grant CS, Barr D, Goellner JR, et al. Benign Hürthle cell tumours of the thyroid: a diagnosis to be trusted? *World J Surg* 1988;12:488–495.
24. Carvalho PA, Chiu ML, Kronauge JF, et al. Subcellular distribution and analysis of technetium-99m-MIBI in isolated perfused rat hearts. *J Nucl Med* 1992;33:1516–1521.
25. Piwnica-Worms D, Kronauge JF, Chiu ML. Uptake and retention of hexakis (2-methoxyisobutylisonitrile) technetium (I) in cultured chick myocardial cells: mito-

chondrial and plasma membrane potential-dependence. *Circulation* 1990;82:1826–1838.
26. Chiu ML, Kronauge JF, Piwnica-Worms D. Effect of mitochondrial and plasma membrane potentials on accumulation of hexakis (2-methoxyisobutylisonitrile) technetium (I) in cultured mouse fibroblasts. *J Nucl Med* 1990;31:1646–1653.
27. Rosai J, Carcangiu ML, Delellis RA. Tumors with oncocytic features (Hürthle cell tumors). In: Rosai J, Carcangiu ML, Delellis RA, eds. *Tumors of the Thyroid Gland*, third series, fasicle 5. Armed Forces Institute of Pathology, Washington, D.C., 1992:161–180.
28. LiVolsi VA. Hürthle cell lesions. In: LiVolsi VA, ed. *Surgical pathology of the thyroid*. Philadelphia: W.B. Saunders; 1990:275–288.
29. Johnson TL, Lloyd RV, Burney RE, et al. Hürthle cell thyroid tumors: an immunohistochemical study. *Cancer* 1987;59:107–112.
30. Albores-Saaveda J, Nadji M, Civantos, et al. Thyroglobulin in carcinoma of the thyroid: an immunohistochemical study. *Hum Pathol* 1983;14:62–66.
31. Dekeyser L, Holyfield L, VanHerle A, et al. Biochemical and immunohistochemical characterization of proteins in Hürthle cell carcinoma. *J Endocrinol Invest* 1984;7:449–454.
32. Vattimo A, Bertelli P, Cintorino M, et al. Identification of Hürthle cell tumor by single-injection, double-phase scintigraphy with technetium-99m-sestamibi. *J Nucl Med* 1995;36:778–782.
33. Vattimo A, Bertelli P, Cintorino M, et al. Double-phase technetium-99m-sestamibi scanning to evaluate nodular thyroid malignancy. *J Nucl Med* 1996;37:1919–1920.
34. Vattimo A, Bertelli P, Burroni L. Effective visualization of suppressed thyroid tissue by means of baseline ^{99m}Tc-methoxy Isobutyl Isonitrile in comparison with ^{99m}Tc-pertechnetate scintigraphy after TSH stimulation. *J Nucl Biol Med* 1992;36:315–318.
35. Gundry SR, Burney RE, Thompson NW, et al. Total thyroidectomy for Hürthle cell neoplasm of the thyroid. *Arch Surg* 1983;118:529–532.
36. Thompson NW, Dunn EL, Batsakis JG, et al. Hürthle cell lesions of the thyroid gland. *Surg Gynecol Obstet* 1974;139:555–560.
37. Miller RH, Estrada R, Sneed WF, et al. Hürthle cell tumors of the thyroid gland. *Laryngoscope* 1983;93:884–886.
38. McDonald RJ, Wu S, Jensen JL, et al. Malignant transformation of a Hürthle cell tumor: case report and survey of the literature. *J Nucl Med* 1991;32:1266–1269.
39. Rossi RL, Nieroda C, Cady B, et al. Malignancies of the thyroid gland: the Lahey clinic experience. *Surg Clin N Am* 1985;65:211–230.
40. Har-El G, Hadar T, Levy R, et al. Hürthle cell carcinoma of the thyroid gland: a tumor of moderate malignancy. *Cancer* 1986;57:1613–1617.
41. Krishnamurthy GT, Blahd WH. Radioiodine ^{131}I therapy in the management of thyroid cancer: a prospective story. *Cancer* 1977;40:195–202.
42. Frazell EL, Duffy BR. Hürthle cell cancer of the thyroid: a review of 40 cases. *Cancer* 1951;4:952–956.
43. Tollefsen HR, Shah JP, Huvos AG. Hürthle cell carcinoma of the thyroid. *Am J Surg* 1975;130:390–394.
44. McLeod MK. Hürthle cell neoplasm of the thyroid. *Otolarygnol Clin NA* 1990;23:441–452.
45. Samaan NA, Shultz PN, Haynie TP, et al. Pulmonary matastasis of differentiated thyroid carcinoma: treatment results in 101 patients. *J Clin Endocrinol Metab* 1985;60:376–380.
46. Hamann A, Gratz K, Soudah B, et al. Szintigraphie mit 131-J bei oxyphilen Karzinomen der Schilddruse. *Nuklearmedizin* 1994;33:219–223.
47. Vergara E, Lastoria S, Varrella P, et al. Technetium-99m-pentavalent dimercaptosuccinic acid uptake in Hürthle cell tumor of the thyroid. *J Nucl Biol Med* 1993;37:65–68.
48. Yen T, Lin H, Lee C, et al. The role of technetium-99m sestamibi whole body scans in diagnosing metastatic Hürthle cell carcinoma of the thyroid gland after total thyroidectomy: a comparison with iodine-131 and thallium-201 whole body scans. *Eur J Nucl Med* 1994;21:980–983.
49. Chia-Hung K, Wan-Yu L, Shyh-Jen W, Shin-Hwa Y. Visualization of suppressed thyroid tissue by ^{99m}Tc-MIBI. *Clin Nucl Med* 1991;16:812–814.

Biologic Dosimetry in Thyroid Cancer Patients After Repeated Treatments with Iodine-131

Radhia M'Kacher, Martin Schlumberger, Jean-Denis Légal, Dominique Violot, Nadine Béron-Gaillard, Anthony Gaussen and Claude Parmentier

Laboratoire de Radioprotection-Médecine Nucléaire, Institut Gustave Roussy, Villejuif, France

To estimate a cumulative dosimetric index that reflects the dose to the circulating lymphocytes after repeated treatments with ^{131}I, biologic dosimetry was applied to 18 patients with differentiated thyroid carcinoma and neck relapse or lung metastases. **Methods:** Chromosomal aberrations were scored in peripheral blood samples that were obtained before and 4 days after each administration of 3.7 GBq ^{131}I according to two methods, conventional cytogenetics and chromosome 4 painting. **Results:** The mean dosimetric index was equal to 0.5 Gy by both methods after the administration of 3.7 GBq ^{131}I. Repeated administrations of ^{131}I delivered the same dose each time, resulting in a cumulative dose from 1–3.5 Gy in the patients who had two to seven treatments. However, the estimated dose, based on the number of chromosomal aberrations on Day 4 and, above all, from the third treatment on, was considerably lower than the real dose absorbed by the lymphocytes. This may be linked to the phenomenon of apoptosis, which results in a loss of information during the course of repeated irradiation. **Conclusion:** Both chromosomal painting and conventional cytogenetics underestimate the cumulative dose after repeated ^{131}I treatments. A complementary test measuring apoptosis may improve the dose estimates.

Key Words: biologic dosimetry; repeated iodine-131 treatments; thyroid cancer

J Nucl Med 1998; 39:825–829

Biologic monitoring of the total-body dose in patients receiving radiation treatment and, in particular, in patients treated with ^{131}I for differentiated thyroid carcinoma is important because its results can guide the subsequent treatment modalities (*1*). Dosimetry is also necessary to establish risk factors due to ^{131}I exposure in these patients and in subjects exposed accidentally to ^{131}I, such as those exposed during the nuclear power plant explosion at Chernobyl (*2*).

Until now, cumulative doses have been derived from numerical estimates based on an approximated geometric model (*3,4*). However, patients treated for differentiated thyroid carcinoma are hypothyroid, and iodine-concentrating metastases may considerably modify the dose to certain organs.

When patients are rendered hypothyroid before treatment, their renal iodine clearance is reduced, which increases the dose to the blood and bone marrow. Until now, no direct measurements have been performed in these patients, nor has there been a follow-up concerning the accumulated dose after repeated treatments with ^{131}I.

Biologic dosimetry seems to be a valuable tool to address this question, even if it supplies only a dosimetric index that reflects the irradiation dose to peripheral lymphocytes (*5*).

The dicentric chromosome is the aberration of choice of biologic dosimetry because its production is almost specific for ionizing radiation and its natural occurrence is low. However, its unsuitability for measuring a dose received some years before the blood sampling is a major drawback (*6,7*). This drawback may now be overcome by scoring stable translocations by fluorescence in situ hybridization (FISH) with whole chromosome probe libraries (*8,9*). The persistence of these radiation-induced translocations may be used for retrospective biologic dosimetry (*10,11*).

In our previous reports (*12,13*), we estimated the dosimetric

Received Dec. 23, 1996; revision accepted Aug. 6, 1997.

For correspondence or reprints contact: Claude Parmentier, MD, Institut Gustave Roussy, 94805 Villejuif Cedex, France.